COMPLEMENTARY VHF CMOS ACTIVE INDUCTOR

A. Thanachayanont and S. Sae Ngow

Faculty of Engineering & Research Centre of Communications and Information Technology
King Mongkut's Institute of Technology Ladkrabang, Bangkok 10520, THAILAND
Tel: +66 2 3269968, Fax: +66 2 7392398, E-mail: ktapinun@kmitl.ac.th

ABSTRACT

A complementary VHF CMOS active inductor is described. The proposed circuit employs 'p-type' and 'n-type' active inductor to obtain enlarged signal handling ability. Under the same inductance, Q value, and power consumption, the proposed circuit shows more than 12-dB improvement in dynamic range while maintaining high-frequency operation. Further enhancement is obtained by using a fully differential floating inductor structure. A 1-GHz 4th-order coupled-resonator filter is designed to demonstrate the potential of the proposed active inductor.

1. INTRODUCTION

Recently, considerable effort has been devoted to the realization of very high frequency active inductor [1]-[5]. Comparing to a typical on-chip spiral inductor, the advantages of an active inductor are large inductance value, high Q, small die area and tuneability. Typically, active inductors are realized by using the classical gyrator-C topology. To achieve very high frequency operation, approaching the f_T of the transistor, the gyrator is realized by using two single-transistor stages and the required integration capacitor is obtained by exploiting the device intrinsic capacitances. Using this approach in modern CMOS technology, one can achieve an inductor self-resonant frequency in the low GHz range. This renders active inductor a viable candidate for IF/RF wireless applications [6]-[8].

However, the limitation of an active inductor is usually on its inability to handle a wide range of signal. This paper presents a complementary CMOS active inductor with improved signal handling ability. Section 2 describes the VHF CMOS active inductor topology. Section 3 describes the proposed complementary inductor and reports its simulated performance. Section 4 presents the design of a 4th-order coupled-resonator bandpass filter using a complementary floating active inductor. Finally, conclusion is given in section 5.

2. VHF CMOS ACTIVE INDUCTOR

Based on the classical gyrator-C topology, two complementary VHF CMOS active inductors that exploit the device intrinsic capacitance are shown in Fig. 1 [2]. Consider a 'p-type' circuit in Fig. 1(a); M_{n1} and M_{p2} realize an active gyrator while the gate-source capacitance of M_{p2} (C_{gs2}) performs the required integration. The circuit simulates a grounded inductor, which appears in parallel with the gate-source capacitance of M_{n1} (C_{gs1}). The equivalent small-signal input impedance Z_{in} is the parallel combination of c_{gs1}, $1/g_{ds2}$, and the impedance Z_L given by eqn. (1).

$$Z_L(j\omega)=\frac{g_{ds1}+j\omega(c_{gs2}+c_{gd1}+c_{gd2})}{(g_{m1}+g_{ds1}+j\omega c_{gd2})(g_{m2}+j\omega(c_{gs2}+c_{gd1}))} \tag{1}$$

The impedance Z_L is approximated by an inductance L_{eq} (i.e. the imaginary part of Z_L) in series with a resistance R_s (i.e. the real part of Z_L) as given by eqns. (2) and (3). The simulated impedance of the circuit in Fig. 1(b) can be derived in the same way.

$$L_{eq}(\omega)=\frac{c_{gs2}}{g_{m1}g_{m2}}\frac{1-\omega^2\frac{c_{gs2}}{g_{m1}g_{m2}}c_{gd2}}{\left(1-\omega^2\frac{c_{gs2}}{g_{m1}g_{m2}}c_{gd2}\right)^2+\omega^2\left(\frac{c_{gs2}}{g_{m2}}+\frac{c_{gd2}}{g_{m1}}\right)} \tag{2}$$

$$R_s(\omega)=\frac{\frac{g_{ds1}}{g_{m1}g_{m2}}+\frac{1}{g_{m1}}\left(1+\frac{g_{m2}}{c_{gs2}}\Big/\frac{g_{m1}}{c_{gd2}}\right)\left(\omega\Big/\frac{g_{m2}}{c_{gs2}}\right)^2}{\left(1-\omega^2\frac{c_{gs2}}{g_{m1}g_{m2}}c_{gd2}\right)^2+\omega^2\left(\frac{c_{gs2}}{g_{m2}}+\frac{c_{gd2}}{g_{m1}}\right)} \tag{3}$$

At frequencies well below the self-resonance, $L_{eq}=c_{gs2}/g_{m1}g_{m2}$ and $R_s=g_{ds1}/g_{m1}g_{m2}$, thus they can be tuned by varying g_{m2} (or g_{m1}) and g_{ds1} respectively. High-Q and wide operating bandwidth active inductors can be realized by reducing g_{ds1}. This can be achieved by applying either cascode or negative resistance cancellation techniques. At high frequencies, close to the self-resonance, R_s rises, and reducing g_{ds1} alone has little effect to the high-frequency loss of the inductor. It can be shown that decreasing g_{ds2} reduces the high-frequency loss of the inductor more effectively [9]. Again this can be obtained by using either cascode or negative resistance cancellation techniques.

The signal handling ability of the circuits in Fig. 1 are limited by the gate overdrive voltage, $V_{gt}=V_{gs}-V_{TH}$. Large V_{gt} is required for good linearity, however this increases supply voltage and power consumption.

3. COMPLEMENTARY VHF ACTIVE INDUCTOR

The 'p-type' and 'n-type' circuits in Fig. 1 can be combined to obtain a complementary active inductor. Note that the resulting circuit is similar to the typical class AB buffer stage. The simulated input impedance of the complementary inductor is the parallel combination of the simulated impedances of the 'p-type' and 'n-type' circuits. To achieve a symmetrical inductor voltage swing, it is important that the 'p-type' and 'n-type' circuits realize the same impedance. This can be obtained by choosing proper transistors' size and bias currents. The advantage of the complementary inductor is increased voltage swing at the cost of larger supply voltage.

The active inductor circuits in Fig. 1(a) and Fig. 2 were simulated by using HSPICE with parameters from a 0.35 μm CMOS technology, and under power supply voltages of 1.5 V and +/- 1.5 V respectively. To obtain a fair comparison, the transistors and bias currents were chosen to attain the same inductance value, Q factor, and power consumption. Table 1 summarizes the simulated performance of the active inductors. The complementary circuit can achieve more than three time increase in voltage swing and 12-dB increase in the dynamic range, comparing to the 'p-type' circuit. This justifies the benefit of the complementary active inductor.

Further dynamic range enhancement can be obtained by using fully differential floating active inductor as shown in Fig. 3, where two complementary circuits are employed. The floating inductor also incorporates cascode and negative resistance devices to enhance the Q value. Fig. 4 shows the Q-enhancement of the inductor, which is obtained by varying V_{c2}. The maximum stable Q that can be obtained is over 2000. Table 1 also summarizes the simulated performance of the complementary floating active inductor.

4. FOURTH-ORDER BANDPASS FILTER

A 4^{th}-order coupled-resonator bandpass filter shown in Fig. 5 was designed to demonstrate the feasibility of the Q-enhanced fully differential floating active inductor. For 1-GHz center frequency and 25-MHz bandwidth, the required component values are: R_S =12 kΩ, R_L =24 kΩ, $C_1 = C_2$ =0.5 pF, C_{12}= 0.01 pF, and $L_1 = L_2$ = 54 nH. The filter dissipates 5.6 mW under +/- 1.5-V supply voltage. Fig. 6 demonstrates tuning of the filter Q by varying Vc2, while Fig. 7 shows the center frequency tuning with gain adjustment of the filter. Note that the filter passband gain is less than the ideal value (i.e. -6 dB) due to the inductor loss. A third-order intermodulation test with two-tone signals at 0.99 and 1.01 GHz showed the filter's in-band third-order input-referred intercept point at –2.5 dBV (see Fig. 9).

5. CONCLUSION

A complementary VHF CMOS active inductor has been described. Simulation results have verified that the proposed complementary inductor can achieve enlarged signal handling ability. Further enhancement has been obtained by using a fully differential floating inductor structure. Overall, the proposed active inductor has improved dynamic range while retaining high frequency and high-Q operation.

Acknowledgements: The financial support of the Thailand Research Fund (PDF/39/2543) and Japan International Cooperation Agency (JICA) are gratefully acknowledged.

6. REFERENCES

[1] A. Karsilayan and R. Schaumann, "A high-frequency high-Q CMOS active inductor with DC bias control," *Proc. 43rd IEEE Midwest Symp. on Circuits and Systems*, pp.486-489, Aug. 2000.

[2] A. Thanachayanont, "A 1.5-V CMOS fully-differential inductorless RF bandpass amplifier," *Proc. IEEE ISCAS'2001*, Vol. 1, pp. 49-52, 2001.

[3] Y. Wu, X. Ding, M. Ismail, and H. Olsson, "Inductorless CMOS RF bandpass filter," *Electronics Letters*, Vol. 37, No. 16, pp. 1027-1028, Aug. 2001.

[4] W. Li, B. L. Ooi, Q. J. Xu, and P. S. Kooi, "High Q active inductor with loss compensation by feedback," *Electronics Letters*, Vol. 35, No. 16, pp. 1328-1329, Aug. 1999.

[5] C. Leifso and J. W. Haslett, "A Fully Integrated Active Inductor with Independent Voltage Tunable Inductance and Series-Loss Resistance," *IEEE Trans. Microwave Theory and Techniques*, Vol. 49, No. 4, pp. 671-676, Apr. 2001

[6] F. Carreto-Castro, J. Silva-Martinez, and R. Murphy-Arteaga, "RF Low-Noise Amplifiers in BiCMOS Technologies," *IEEE Trans. Circuits and Syst.-II*, Vol.46, No. 7, pp. 974-977, Jul. 1999.

[7] E. Säckinger and W. C. Fischer, "A 3-GHz 32-dB CMOS Limiting Amplifier for SONET OC-48 Receivers," *IEEE J. Solid-State Circuits*, Vol. 35, No. 12, pp. 1884-1888, Dec. 2000.

[8] J. van der Tang, D. Kasperkovitz, and A. van Roermund, "A 9.8-11.5 GHz quadrature ring oscillator for optical receivers," *Proc. IEEE CICC 2001*, pp.323-326.

[9] A. Thanachayanont and A. Payne, "CMOS floating active inductor and its applications to bandpass filter and oscillator designs," *IEE Procs. Circuits, Devices and Systems*, Vol. 147, No. 1, pp. 42 –48, Feb. 2000.

Table 1. *Simulated Performance of the active inductors*

Parameters	Fig. 1(a)	Fig. 2	Fig. 3
V_{DD} (V)	1.5	+/- 1.5	+/- 1.5
P_{diss} (mW)	1.7	1.7	2.76
f_o (GHz)	4.14	4.45	2.6
[1]L (nH)	15.11	15.67	51.5
[1]Q (at 1 GHz)	3	3.4	126
[2]Noise (μV)	108	104	134
[1,3]Max. V_L (mV)	2	7.45	67.6
Dynamic range (dB)	25.4	37.1	54

[1]at 1 GHz, [2]integrated over 500 MHz bandwidth, [3]THD < 1 %

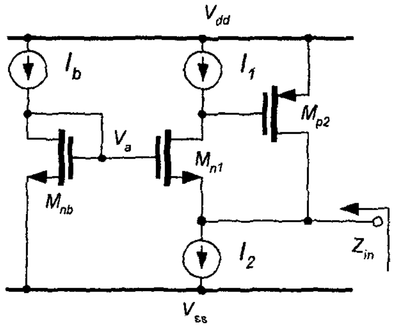

(a)

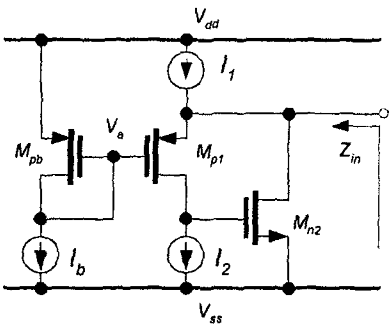

(b)

Figure 1. VHF CMOS active inductors.

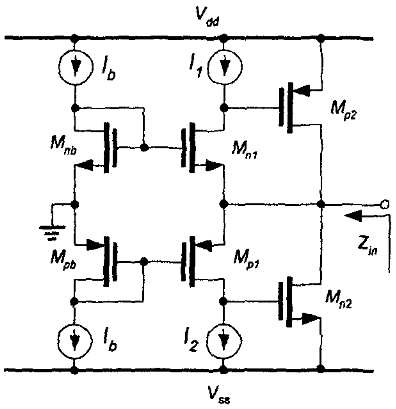

Figure 2. Complementary VHF active inductor.

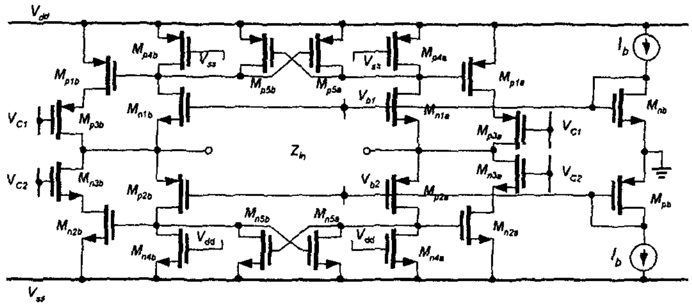

Figure 3. Q-enhanced complementary fully differential floating active inductor.

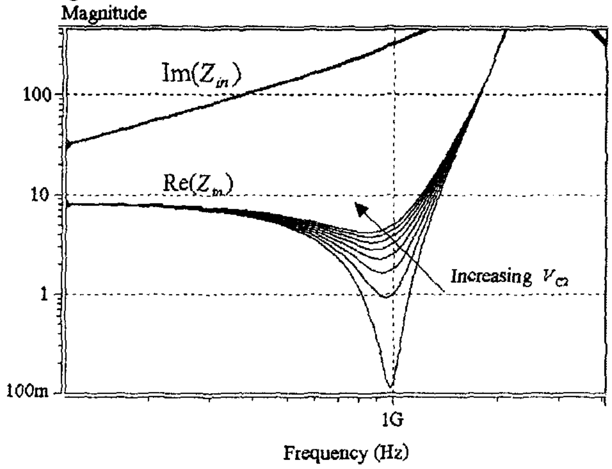

Figure 4. Q-tuning of the active inductor.

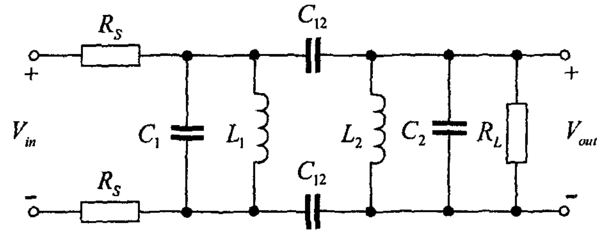

Figure 5. 4[th]-order coupled-resonator bandpass filter.

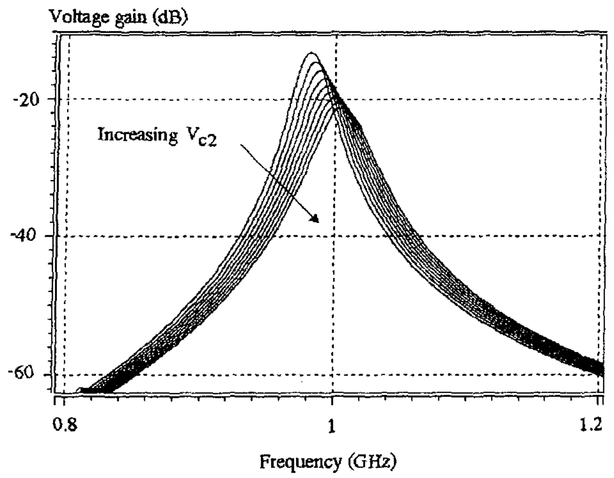

Figure 6. Q-tuning of the bandpass filter.

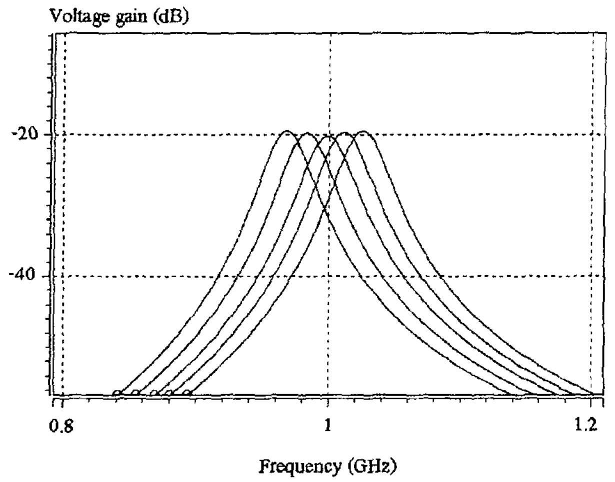

Figure 7. Centre frequency tuning with gain adjustment of the filter

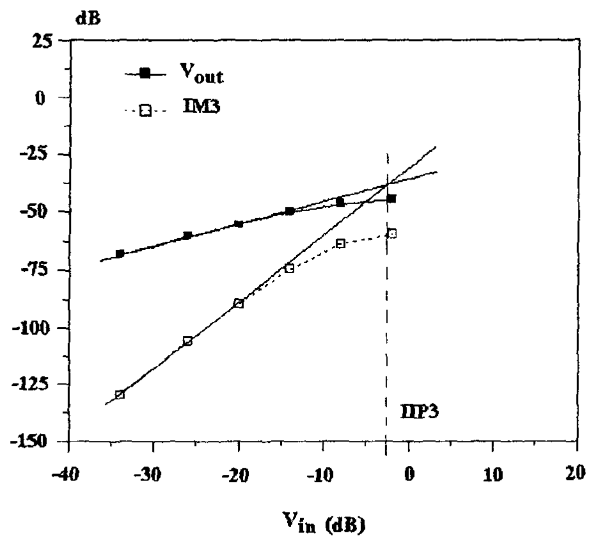

Figure 8. 3rd-order intermodulation of the filter.